ISSN 1855-9913

Journal of the Laser and Health Academy
Vol. 2020, No.1; www.laserandhealth.com

Influence of Different Absorption in Desiccated Tissue on Soft-Tissue Surgery with Er:YAG and CO_2 Lasers

Matjaz Lukac[1], Jernej Kukovic[2], Nejc Lukac[3], Franci Bajd[4]
[1]Institut Jozef Stefan, Jamova 39, 1000 Ljubljana, Slovenia
[2]University Medical Centre Ljubljana, Department of Dermatovenereology, Zaloska 2, 1000 Ljubljana, Slovenia
[3]Fotona d.o.o., Stegne 7, 1000 Ljubljana, Slovenia
[4]University of Ljubljana, Faculty of Physics and Mathematics, Jadranska 19, 1000 Ljubljana, Slovenia

ABSTRACT

In this study, we examined and reviewed the effect of laser wavelength on the cutting rate and peripheral thermal damage during soft-tissue surgery with mid-IR Er:YAG (2,940 nm) and CO_2 (9,000-11,000 nm) lasers.

In agreement with published experimental data, our analysis of the Er:YAG and CO_2 laser-tissue interaction demonstrates that the ablative and thermal diffusion effects on soft human tissues are very similar for both laser types. This is attributed to the fact that both lasers are predominantly strongly absorbed in the soft tissue's intrinsic water content, resulting in the same basic mechanism of interaction with soft tissues which is based on a micro-explosive "boiling" of the confined intrinsic water.

However, as the laser-heated tissue gets partially or completely desiccated during surgery the two laser wavelengths start exhibiting very different properties. While tissue desiccation merely reduces the cutting speed of the Er:YAG laser, the CO_2 laser's higher absorption in the residual dry substance can in addition lead to very high tissue temperatures accompanied by tissue charring. For this reason, CO_2 laser surgery is more often accompanied by a higher level of thermal injury to the surrounding tissues, with charring and melting of wound margins, especially at lower volume power densities. This may promote tissue defragmentation and frequently makes histopathological evaluation impossible.

Key words: Er:YAG, CO_2, laser, soft tissue surgery, ablation, coagulation

Article: J. LA&HA, Vol. 2020, No.1; pp. 1- 11.
Received: March, 2018; Accepted and published: January, 2019;
Re-published in abbreviated version online first August 8, 2020.

I. INTRODUCTION

Human tissues are multi-component composite systems, with generally very complex interactions with laser light. Within the UVB (280-320 nm), UVA (320-400 nm) and visible light (400-700 nm) spectral regions, skin has three primary absorbers: blood (hemoglobin), melanosomes (melanin), and keratin (see Fig. 1) [1, 2].

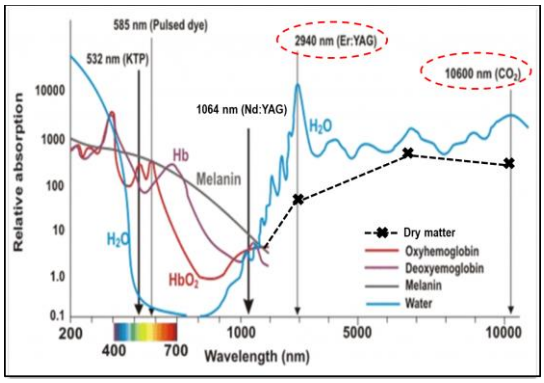

Fig. 1: Absorption spectra of human soft tissues. The highest absorption peaks are at the Er:YAG (2,940 nm) and CO_2 (10,640 nm) laser wavelengths. The crosses represent approximate data for dry matter (desiccated tissue) [2-4]; the dotted line is a guide to the eye only.

Despite its abundance in all tissues, water is not a significant absorber of light in the visible region. However, above approximately 1000 nm it becomes a primary absorber, considerably simplifying the interaction mechanism. The ability of mid-infrared lasers to incise and excise soft tissue is thus mainly due to the significant optical absorption of water content (60~80%) in soft human tissues [5].

Ablation temperatures above 100 ^{0}C [6-8], as well as the dependence of ablation efficiency on tissue tensile strength [9], and histological evidence of tissue tear [6] all indicate that the ablation of soft tissue with mid-IR lasers is not purely a water evaporation process. Supported also by observations from high-speed photography [10, 11] and time-resolved thermometry [9], a mechanism of micro-explosions is now generally accepted as the main thermo-

mechanical mechanism of ablation of soft tissues with mid-IR lasers [12]. As the tissue water, which is trapped within the microscopic cavities within the soft tissue, absorbs the laser radiation, its temperature increases linearly until the boiling point ($T \approx 100\ ^0C$) is reached. Further heating converts one part of the water mass into vapor. As the vapor cannot expand freely, pressure in the cavity rises and exerts force on the cavity wall. Micro-explosive removal of tissue starts when the pressure exceeds the ultimate tensile strength of the tissue, which for soft tissues occurs at water vapor temperatures of about $250\ ^0C$ [7, 13, 14].

Among mid-infrared lasers, the CO_2 (9,000-11,000 nm) and Er:YAG (2,940 nm) lasers are most suitable for performing soft-tissue surgery since their wavelengths are located at the two highest water absorption peaks (Fig. 1). The optical penetration depth (δ_{opt}) of both laser types in soft tissues is very small, below 20 μm (≈3 μm for Er:YAG and ≈ 17 μm for CO_2) [14].

In this analysis, we compare the ablative and peripheral thermal coagulation effects of the Er:YAG (2,940 nm) and CO_2 (10,640 nm) lasers on soft human tissues such as skin or mucosa. The comparison is made based on numerical calculations using the micro-explosions model of mid-infrared laser ablation of soft tissues [12-15], and on the published in-vitro, ex-vivo and in-vivo studies.

II. MATERIALS AND METHODS

In our study, we applied a numerical model of the physical process of tissue resurfacing as originally developed to study thermo-mechanical ablation with mid-IR lasers. The details of the model are described in [12-15], and will not be repeated here.

In the model, a single wavelength (λ = 2,940 nm or λ = 10,640 nm) of continuous wave (CW) or pulsed laser radiation with power P (in W) is delivered to the surface area (S) of the treated tissue with a surface power density $P_d = P/S$ (in W/cm^2) or pulse fluence F (in J/cm^2). For a circularly shaped irradiated area, $S = \pi\ d^2/4$, where d is the diameter (spot size) of the irradiated area. We modelled the tissue as a water-containing homogeneous media characterized by a single absorption coefficient of $k = 1/\delta_{opt}$ for the delivered Er:YAG or CO_2 laser wavelength λ. Assuming a 70% water content of the modelled soft tissue, the optical penetration depths were taken to be 3 μm for Er:YAG and 17 μm for CO_2. Since the main focus of our study was on the Er:YAG and CO_2 laser wavelengths with their very short penetration depths, the effects of the scattering of laser light within the tissue were not included. Similarly, it was taken that the laser spot size (d) is much larger than the optical penetration depth (δ_{opt}) and, therefore, the diffusion of dissipated heat was treated in one dimension using a finite-difference scheme. Our model accounted for the fact that a substantial amount of the incident beam energy (approximately a half) is expected to be lost at the air-tissue boundary on account of refractive index differences.

The model enabled the calculation of the temporal evolution of the tissue temperature during and following laser irradiation of different laser modalities (CW or pulsed) for different depths z within the tissue, calculated from the extrapolated thermal gradient.

The tissue surface is treated as perfectly insulated. This is accomplished by introducing an additional spatial point just outside the tissue surface with the temperature equal to the value at the neighboring superficial point, thus preventing any heat flow through the surface. When the pressure p exceeds the ultimate tensile strength of the tissue, the ablation of tissue begins. The depth to which the tissue gets ablated is denoted by d_{abl} (in μm).

According to the thermo-mechanical ablation model [12-15], a one-dimensional temperature field was updated at each simulation time step by using a compact three-point stencil discretization approach that provided a fast, yet sufficiently accurate calculation of the temperature field change upon the delivery of laser pulse irradiation. The light-tissue interaction was modeled by using Beer's law. Stability of the numerical integration scheme was provided by choosing a sufficiently high spatial resolution equal to $\Delta z = 0.12\ \delta_{opt}$ (0.4 μm and 20 μm for Er:YAG and CO_2, respectively) as well as by the temporal resolution Δt that was determined by the Courant–Friedrichs–Lewy number equal to 0.45. The accuracy of the temperature field calculation could be slightly further improved by additionally increasing the spatial resolution, at the expense of a substantially increased computational load. In the study, the following laser parameters were used: pulse duration of t_p = 1000/1500 μs with pulsed mode, or t_p = 0.3/1 s with CW mode, pulse repetition rate f = 20/50 Hz, maximal simulation time of 1 s. In the simulations, fluence values were chosen in order to obtain the maximal surface power densities up to 600 W/cm^2. For each simulation run, the response of the model tissue was characterized by the ablation depth as a function of time (acquired at each Δt) and the instantaneous temperature field (acquired at each 1000 Δt), from which the ablation speed and the depth of heat penetration were calculated. The following tissue properties were assumed in the model: tissue density ρ =

1100 kg/m³, specific heat of the tissue's solid component c_s = 1700 J/kgK, specific heat of water c_w = 4200 J/kgK, tissue specific heat $c_m \approx$ 3500 J/kgK and tissue thermal conductivity λ_{th} = 0.42 W/mK.

III. RESULTS

a) Ablation rate

The calculated ablation (cutting) speed AS = d_{abl}/time (in μm/s) for CO_2 and Er:YAG lasers operating in continuous wave (CW) or pulsed (pulse duration t_p = 1500 μs, pulse repetition rate f = 20 or 50 Hz) mode are shown in Fig. 2.

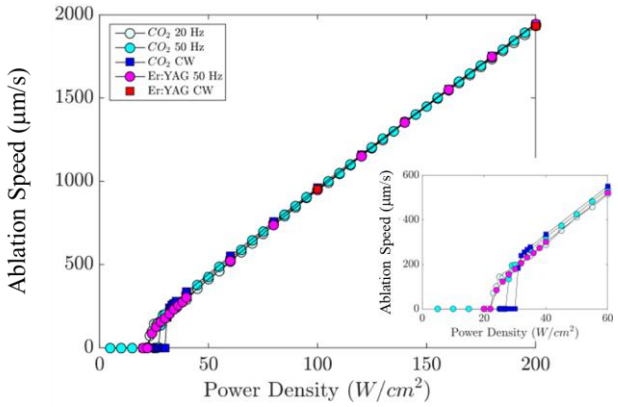

Fig. 2: Calculated ablation speed (AS) versus surface power density for CW (squares) and pulsed (circles) operation of Er:YAG and CO_2 laser. Note the similarity of ablation speeds for the two laser sources and for different laser irradiation modes.

As can be seen from Fig. 2, the more than 5-fold difference in the optical penetration depths between the two laser sources does not have a significant influence on the ablation rate AR = AS/P_d (in μm/(J/cm²)) in soft tissues. Within the micro-explosions boiling model, the ablative effect on soft tissue is the same for Er:YAG and CO_2 laser wavelengths. Similarly, the soft-tissue average cutting speed does not depend on whether the laser energy is delivered in a continuous (CW) or pulsed manner. Therefore, the above figure can be considered to also represent the dependence of the ablation depth d_{abl} (in μm) on the laser pulse fluence F (in J/cm²).

Note that the speed of mass removal, MS (in g/s) is proportional to the laser power P as:

$$MS = P\,(AR\,\rho\,S) \quad . \tag{1}$$

The similarity of the slopes of the ablation rates AR = AS/P_d = d_{abl}/F, (in μm/(J/cm²)) of the two laser types was also observed experimentally [16]. Figure 3 depicts the measured dependence of the ablation depth vs. fluence for the ablation of guinea pig skin using a TEA CO_2 laser and a normal-spiking-mode Er:YAG laser.

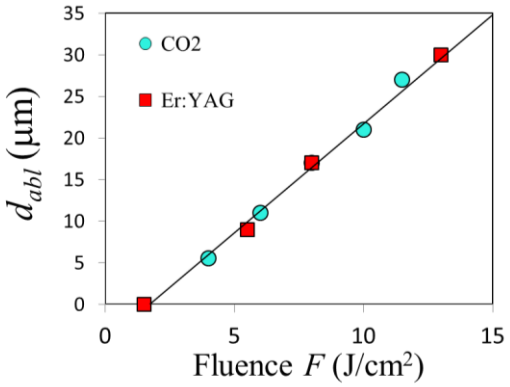

Fig. 3: Measured ablation depth vs. fluence for the ablation of guinea pig skin using a CO_2 (t_p = 2μs) and an Er:YAG laser (t_p = 250 μs) [16]. Note the similar ablation rates for these two different sources of infrared laser radiation.

The observed similarity of the ablation rates of Er:YAG and CO_2 lasers confirms that confined "boiling" with micro-explosions is the main ablation mechanism for both laser types, despite the difference between their absorption coefficients.

Our model predicts the CO_2 and Er:YAG laser ablation rates in soft tissues of approximately $AR \approx$ 5 μm.cm² J⁻¹. This is in good agreement with the reported measured ablation rates for CO_2 and Er:YAG in soft tissues ranging between 2 and 4 μm.cm².J⁻¹ [15-20]. Slightly lower measured ablation rates than calculated can be attributed to the effect of tissue desiccation during laser irradiation, and partially also to additional heat losses not included in our model. Such losses include, for example, heat diffusion in the transverse direction and heat flow into the surrounding.

Finally, the independence of the ablation rate on the optical penetration depth can also be concluded based on analytical relations. It is well known that in the absence of heat diffusion, the ablation threshold fluence (F_{th}) can be calculated from [21]:

$$F_{th} = h_a \,.\, \delta_{opt} \,, \tag{2}$$

where h_a marks the specific heat of ablation (in J/mm³). The ablation threshold fluence represents the fluence required to ablate a tissue layer with a thickness δ_{opt}. When a tissue is irradiated with a certain laser surface power density P_d, a tissue layer with thickness δ_{opt} gets heated up to the ablation threshold in the ablation time t_{abl}, defined by $F_{th} = P_d\, t_{abl}$ [21], and therefore:

$$t_{abl} = h_a \,.\, \delta_{opt} / P_d \,. \tag{3}$$

Finally, this gives the ablation speed AS that is independent of the laser wavelength:

$$AS = \delta_{opt} / t_{abl} = P_d / h_a \,. \quad (4)$$

By taking $h_a \approx$ 3-4 J/mm^3 [15, 22], we obtain the ablation rate of $AR \approx 3$ µm.cm^2 J^{-1}, in good agreement with our numerical calculations and published measurements.

In what follows, we shall assume the ablation rate for both lasers to be $AR = 3$ (µm/s)/(W/cm^2), which represents an approximate average of the reported ablation rates for both laser types.

b) Thermal depth

The Er:YAG and CO_2 lasers are generally considered to be ablative lasers due to their very high absorption in water, and the resulting very short optical penetration depth (δ_{opt}) into human tissues. However, it is not only the optical penetration depth but also the depth of thermal diffusion (δ_{diff}) that takes place during a laser irradiation of duration t_{ir} that determines the thermal penetration depth (d_{th}) of the laser radiation: $d_{th} = \delta_{opt} + \delta_{diff}$ [21]. In this study, we calculated d_{th} as the depth within the tissue at which the temperature increase ΔT caused by laser irradiation drops to 50% of the temperature increase at the surface of the tissue. Our model calculations show that the thermal diffusion depth (δ_{diff}) can be roughly estimated from the characteristic diffusion depth $\delta_{diff} = 0.5\ (2D\ t_{ir})^{1/2}$ (the pre-factor of 0.5 accounting for the half-space geometry of the model), in which the diffusion constant $D = \lambda_{th}/\rho c_m$ for the skin is equal to 1.1 x 10^{-7} m^2/s [12].

Our analysis shows that there are three, basically simultaneous steps in tissue heating upon laser irradiation [21]. The tissue is first heated directly within the optical absorption depth (*direct heating*) (Fig. 4 a). Direct heating is followed by thermal diffusion that indirectly heats the deeper lying tissues (*indirect heating*) (Fig. 4 b). For short irradiations, the time span for thermal diffusion is short, and the heat energy does not reach very deep into the tissue. For longer irradiations, the heat has sufficient time to spread deeper into the tissue. In the third step, the hottest part of the tissue close to the surface is ablated, in effect reducing the depth of the thermally affected skin layer (Fig. 4 c).

Therefore, the longer the duration of laser irradiation (t_{ir}), the longer the thermal diffusion depth (δ_{diff}), and consequently also the longer the overall thermal penetration depth (d_{th}). This can be seen in Fig. 5, which shows the dependence of the thermal penetration depth on the laser irradiation time in the absence of ablation.

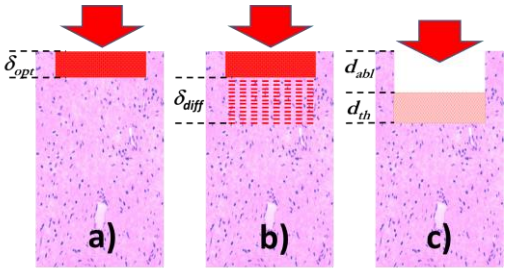

Fig. 4: Three steps in tissue heating upon laser irradiation: a) tissue is first heated directly within the optical absorption depth (*direct heating*); b) direct heating is followed by thermal diffusion that indirectly heats the deeper lying tissues (*indirect heating*); and c) ablation of the hottest part of the tissue close to the surface.

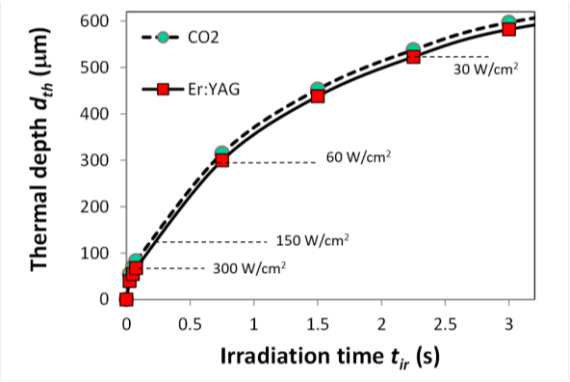

Fig. 5: Dependence of thermal depth on irradiation time in the absence of ablation. The dotted horizontal lines mark the maximal thermal depths achievable with different power densities.

On the other hand, the higher the ablation speed, the shorter the overall thermal depth, since at higher ablation rates most of the thermally affected layer is being removed by means of micro-explosions. This can be seen in Fig. 6, which shows the dependence of the thermal depth on the power density for $t_{ir} = 0.3$ s.

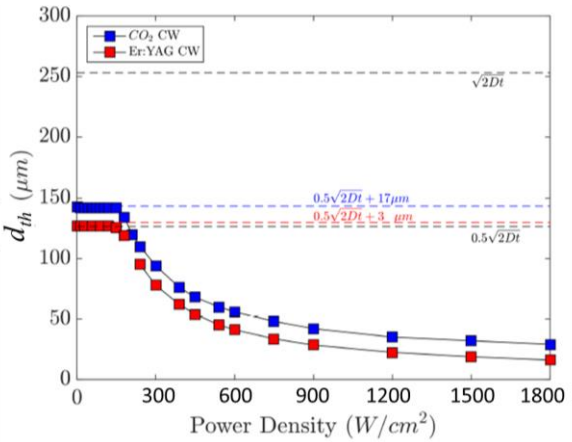

Fig. 6: Thermal depth as a function of surface power density for irradiation time of $t_{ir} = 0.3$ s, comparatively for CO_2 and Er:YAG.

For any laser power density, the thermal depth will increase with time following the onset of laser

irradiation until the ablation threshold is reached, after which the confined boiling with micro-explosions will prevent the thermal depth from increasing any further (See Fig. 7). This maximal thermal depth depends on the surface power density, being smaller for higher surface power densities (see Fig. 8).

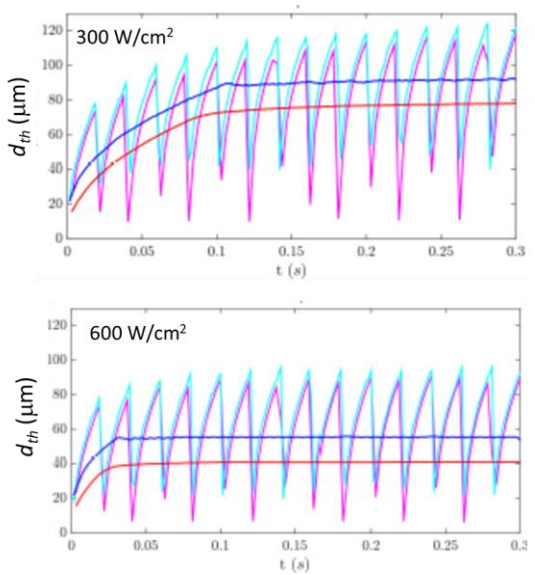

Fig. 7: Temporal evolution of the thermal depth for P_d = 300 W/cm² (above) and P_d = 600 W/cm² (below) for CW Er:YAG (red) and CO_2 (blue) mode, and for pulsed (t_p= 1.5 ms, 20 Hz) Er:YAG (violet) and CO_2 (cyan) mode.

Note that when the laser energy is delivered in a repetitive pulsed mode, the instantaneous laser power densities during a pulse are much higher than the power density averaged over the pulses. This results in a "pulsed" ablation and an oscillation of the thermal depth around the maximal thermal depth of the corresponding CW mode with the same average power density P_d. (see Fig. 7).

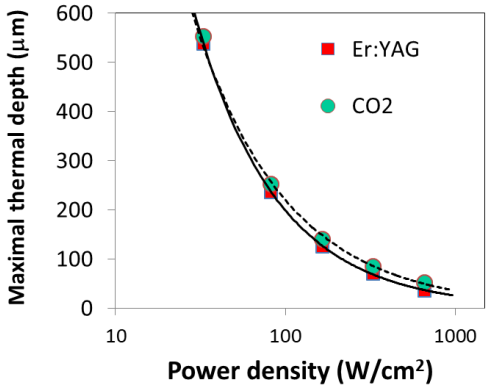

Fig. 8: Maximal thermal depth as a function of surface power density. The higher ablation speed at higher power densities reduces the overall depth of the thermally affected tissue layer.

As can be seen from the above figures, the thermal depths resulting from the combined effect of thermal diffusion and ablation are approximately the same for Er:YAG and CO_2 lasers, regardless of whether the laser radiation is delivered in a CW or pulsed mode. Note that the calculated thermal depths coincide well with the measured depths of thermal damage of ≈ 50 - 100 µm, as observed during cutaneous surgery with Er:YAG and CO_2 lasers [20, 22].

c) Tissue desiccation

The water content of soft tissues is very high, and varies between 65 and 80% [5]. However, it is well known that as a result of laser heating, the tissue can get progressively desiccated, leading to a significant reduction in tissue water content [23, 24]. Our measurements of the surface temperature on agar following irradiation with a single Er:YAG laser pulse show that the temperature does not grow linearly with the laser fluence up to the ablation threshold, but exhibits a slight bend at an intermediate temperature (see Fig. 9a). Agar with 70% water content was used, assuming its optical and thermo-mechanical properties to be close to those of soft tissues. Similar measurements with CO_2 and Er:YAG lasers have been made also on human skin [7, 25]. In agreement with our measurements in agar, they showed a bend occurring at about 100 ^{0}C (Fig. 9 b). This behavior was attributed to the accelerated process of evaporation of the heated soft tissue's free water, effectively desiccating the tissue already during a single laser pulse.

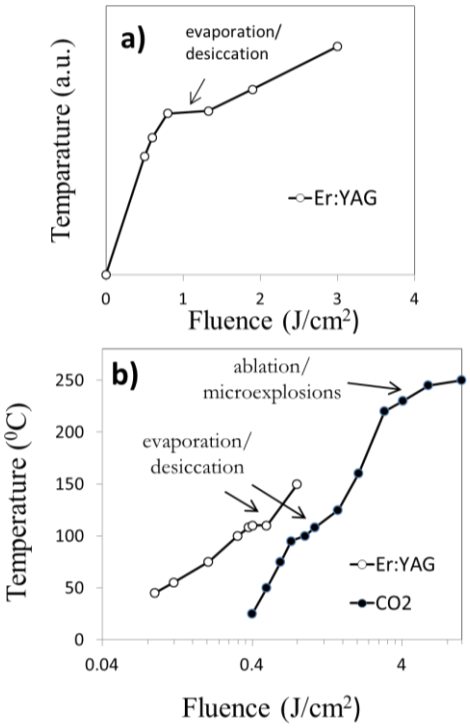

Fig. 9: Measured dependence of the surface temperature on the laser fluence for a) Er:YAG laser on agar; and b) Er:YAG and CO_2 laser on human skin [7]. The intermediate bend in the temperature curve is caused by the evaporation of free water within the tissue.

Therefore, in the initial heating phase the free water starts to evaporate, followed in the next stage by the micro-explosive confined boiling of the bound water. Water evaporation was observed also during ablation studies with a CO_2 laser on guinea pig skin by measuring the tissue mass before, during and after laser irradiation [18]. The measured mass loss rate due to incidental water evaporation was negligible prior to laser irradiation, became appreciable during laser heating and ablation, and continued also after the laser radiation was stopped (see Fig. 10).

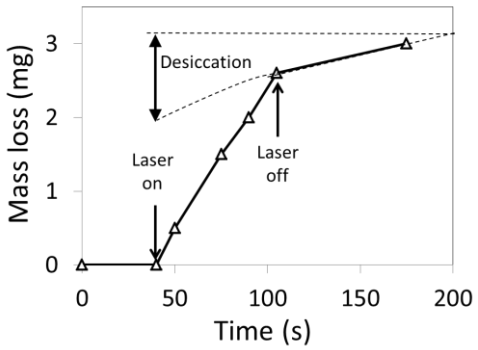

Fig. 10: Tissue mass versus time prior, during and post CO_2 laser irradiation of guinea pig skin [18]. Note that the pre-ablation evaporation rate is negligible, while the post-ablation evaporation rate is considerable due to the tissue temperature remaining elevated, and the superficial dry stratum corneum having been ablated.

The phenomenon of tissue desiccation has an especially pronounced effect on the ablation of hard tissues with low intrinsic water content [26]. For example, Fig. 11 shows a progressive reduction in the measured ablation depth with the increasing number (N) of successively delivered Er:YAG laser pulses on enamel (3% water content) and cementum (22% water content) [27].

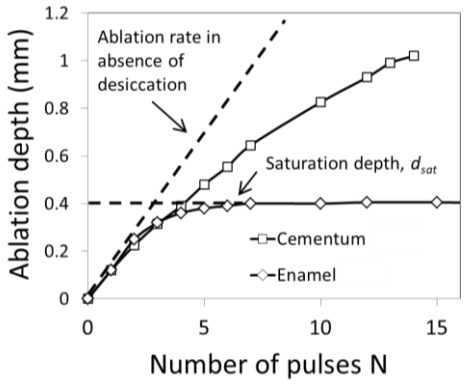

Fig. 11: Measured ablation depths in enamel and cementum as a function of delivered laser pulses N, for the same Er:YAG laser pulse fluence of $F = 35$ J/cm^2 [27].

As a result of tissue desiccation, considerable reduction and even stalling of the ablation process occurs during the delivery of consecutive Er:YAG laser pulses on cementum and enamel. The effect is most pronounced on enamel, the human tissue with the lowest water content (3%). The ablation on enamel starts with a relatively high intrinsic ablation rate and as the enamel gets progressively desiccated, the ablation stalls at the ablation saturation depth, d_{sat}. However, a considerable reduction in the ablation rate is observed also on cementum (22% water content).

It is important to note that in order to improve the measurement sensitivity, the ablation rates are typically measured from the depth, volume or mass of cavities made by a large number of consecutively delivered pulses, or by a prolonged delivery of CW laser irradiation [26, 27]. As a result, the measured ablation rates are typically lower than what would be the intrinsic ablation rates in the absence of tissue desiccation [27-29].

Ignoring the effects of thermal diffusion, the time available for tissue desiccation (t_{des}) is equal to the ablation time t_{abl}, i.e. the time required for the laser to heat up the tissue layer of thickness δ_{opt} up to the ablation threshold (see Eq. 3). While the optical absorption depth does not affect the ablation speed, $AS = \delta_{opt}/t_{abl} = \delta_{opt}/t_{des}$, it does affect the time required for the tissue to be heated up to ablation. The longer the desiccation time, the more free water gets evaporated and the more likely it is that the water micro-explosive mechanism will be overcome by the mechanism of melting of the dried out tissue. As follows from Eq. 3, the desiccation time is not fully defined by the surface power density, but by the volume power density, $P_v = P_d/\delta_{opt} = P/(S\delta_{opt})$ (in W/mm^3):

$$t_{des} = h_a / P_v \quad . \tag{5}$$

The higher the volume power density, the shorter the desiccation time and consequently also the lower the level of tissue dehydration (see Fig. 12). This has been confirmed also experimentally. For example, the CO_2 laser ablation rate in guinea pig skin was measured to increase by a factor of 1.6 when the volume power density was increased from 64 to 6400 W/mm^3 [19], as expected from the lower level of tissue dehydration at the higher power density. Similarly, charring caused by tissue desiccation was reported to occur more readily at lower CO_2 laser power densities [78, 80].

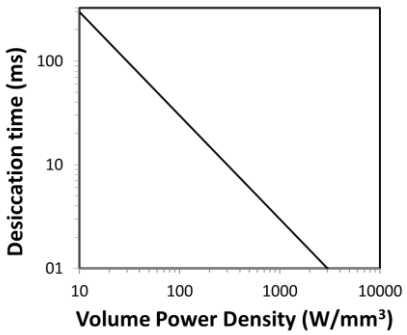

Fig. 12: Dependence of desiccation time t_{des} on volume power density P_v.

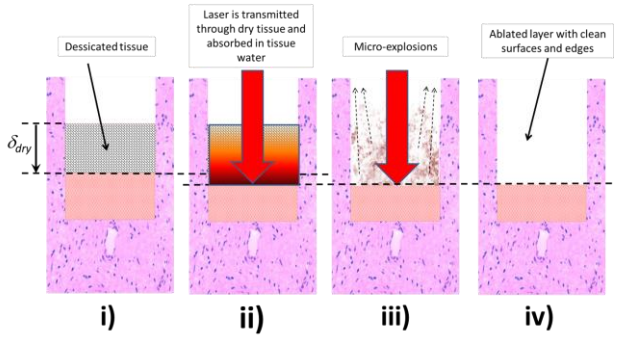

Fig. 13: Depiction of the water mediated micro-explosive ablation mechanism for Er:YAG in partially desiccated soft tissue.

IV. DISCUSSION

a) Effects of tissue desiccation

Our analysis of the Er:YAG and CO_2 laser-tissue interaction demonstrates, in agreement with published experimental data, that the ablative and thermal effects on soft human tissues are very similar for both laser types. This is attributed to the fact that both lasers are predominantly strongly absorbed in the soft tissue's intrinsic water, resulting in the same basic mechanism of interaction with soft tissues. During rapid heating of the confined tissue water, high subsurface pressures are created that lead to the explosive removal of the surrounding tissue material.

Soft-tissue desiccation during laser surgery with mid-IR lasers is an undesirable phenomenon since it reduces the cutting efficacy. Therefore, it is desired that laser parameters and surgical protocols are chosen such that this effect is minimized. However, in general, it does not have a detrimental effect on surgical laser procedures on soft tissues. An exception is procedures on hard tissues that are characterized by low water content, where external water spray needs to be delivered onto the irradiated area in order to re-hydrate the tissue to prevent complete ablation stalling [27-29].

The above considerations apply only for mid-IR wavelengths, where the difference is relatively high between their predominant absorption in water and the underlying absorption in dry substance. In this case, the water micro-explosive mechanism continues to dominate even under partial desiccation conditions (see Fig. 13)

However, when the difference between the absorption in water and dry tissue is relatively small, then even a small level of desiccation can cause the water micro-explosive mechanism to be replaced by the mechanism of melting, carbonization and evaporation of the dry matter (see Fig. 14). This is because in such situations there is no longer an adequate water heat sink to hold the temperature at the water's boiling temperature.

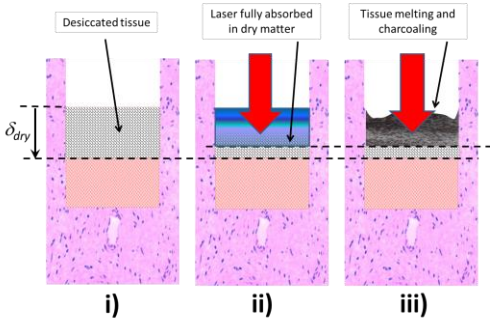

Fig. 14: Depiction of the melting with charring ablation mechanism for CO_2 in partially desiccated soft tissue.

For example, in dental dentin (12% water content) the absorption of Er:YAG (2,940 nm) in the hydrated tissue is approx. 10 times higher than in the desiccated tissue, while for the Er,Cr:YSGG laser (2,730 nm) this ratio is about 3-times smaller [30]. In the absence of water spray, this difference results in carbonized cavities with Er,Cr:YSGG, while clean cavities are achieved with Er:YAG, in spite of the dentin getting desiccated in both cases (Fig. 15) [31].

Fig. 15: Pictures of cavities in dentin, made with Er:YAG and Er,Cr:YSGG lasers following three consecutive laser pulses of the same laser pulse fluence and duration [31].

A similar effect is observed also in soft-tissue surgery with Er:YAG and CO_2 lasers. In this case, the absorption of Er:YAG (2,940 nm) in the hydrated soft tissue is approx. 300 times higher than in the desiccated tissue, while for the CO_2 laser (10,640 nm) this ratio is much smaller, only about 8-times [4]. Therefore, the amount of light absorption in desiccated tissue for the Er:YAG laser is virtually negligible, while for the CO_2 laser interaction, the absorption in the desiccated tissue can be considerable. Assuming that desiccation occurs within the thermal depth, a rough estimate shows that a complete absorption of the CO_2 laser energy by the dry substance will occur within a typical thermal depth of 100 μm. On the other hand, for the Er:YAG laser to be completely absorbed within the desiccated tissue layer, the thermal depth should be much larger, on the order of 900 μm. Consequently, tissue denaturation and charring occurs much more readily during CO_2 soft-tissue surgery.

Soft-tissue ablation is thus governed by the interplay of two opposing effects. On one hand, higher surface power density reduces the desirable thermal depth (See Fig. 8), while on the other hand, higher power density decreases the level of tissue desiccation (See Eq. 5). It is to be noted that for the same surface power density, the volume power density of the Er:YAG laser is about 6 times larger than that of the CO_2 laser, due to the difference in their optical penetration depths. Therefore, for the same surface power density, the tissue gets desiccated faster when irradiated by the CO_2 laser (See Eq. 5). Surgeons using CO_2 laser are therefore advised to avoid using low surface power densities because they cause carbonization [80].

The calculated dependence of the desiccation time on the laser type (optical penetration depth) and surface power density is presented in Table 1.

Table 1: Dependence of volume power density P_v, and consequently of desiccation time (t_{des}) on surface power density, P_a. For the same surface power density, the time available for desiccation is higher with the CO_2 laser.

	CO2		Er:YAG	
Surface Power Density (W/cm^2)	Volume Power Density (W/mm^3)	Desication time (in ms)	Volume Power Density (W/mm^3)	Desication time (in ms)
50	29	102.0	167	18.0
100	59	51.0	333	9.0
200	118	25.5	667	4.5
500	294	10.2	1667	1.8
1000	588	5.1	3333	0.9
2000	1176	2.6	6667	0.5
5000	2941	1.0	16667	0.2
10000	5882	0.5	33333	0.1

Experiments show that observable desiccation occurs already for CO_2 laser pulses with t_p = 2 ms [7, 25]. Therefore, in order to avoid excessive desiccation and charring, it is recommended that CO_2 laser surgery is performed at higher surface power densities than with Er:YAG [80], in order to obtain approximately the same or preferably higher volume power density with the CO_2 laser.

A strong hemostatic effect is often reported for the CO_2 laser [42, 43], which can be attributed to tissue desiccation and the associated tissue overheating and charring [78, 80]. While the hemostatic effect of the CO_2 laser as a result of tissue desiccation may be welcome [20], it can also lead to higher post-operative morbidity and complications. It is important to note that excessive thermal injury and damage not only produces erythema, but it can also be associated with angiogenesis, leading to visible telangiectasia, potential hypertrophic scarring and the development of late hypopigmentation [38-41].

As has been shown, the Er:YAG laser the hemostatic and ablative effects can be controllably generated without the risk of charring by appropriately adjusting the laser parameters [35, 44]. When low fluences (below or around the ablation threshold ~ 1 J/cm^2; see Fig. 3) and low average surface power densities (below approx. 200 W/cm^2; see Figs. 5 and 8) are applied to the tissue, strong coagulation effects are observed [35]. Therefore higher fluences (2–5 J/cm^2) are used for tissue ablation and lower fluences (≤ 1 J/cm^2) for tissue coagulation (see Fig. 3). This can be, for example, simply achieved by changing the laser spot size from small (for ablative high fluences) to large (for coagulative small fluences) by manually adjusting the distance between the treated tissue and the focal point of the surgical handpiece [35]. The ability to use the Er:YAG laser in the ablation or coagulation mode (as needed) without the risk of charring is one of its unique advantages.

V. CONCLUSIONS

Our study shows that in spite of their large difference in wavelengths, the Er:YAG (2,940 nm) and CO_2 (9,000-11,000 nm) lasers are very similar in terms of their ablation rates and the thermal-diffusion generated peripheral coagulation at the ablation site during soft-tissue surgery. This is because both lasers are predominantly absorbed by the intrinsic tissue water within a very shallow tissue depth of less than 20 μm, and therefore their ablative and thermal effects are governed by the same laser-tissue interaction mechanism of micro-explosive "boiling" of the confined tissue water.

The micro-explosive "boiling" of the confined tissue water results in clean cuts without any undesirable excessive thermal damage of the soft tissues [32-35]. Therefore, it is imperative that no significant tissue desiccation occurs during a procedure. Otherwise, tissue overheating with accompanying undesirable carbonization can occur [16, 22, 36, 37, 78, 80]. Here, the Er:YAG is at a significant advantage due to its larger difference between the absorption in the intrinsic water and dry substance. Consequently, undesirable tissue desiccation with resulting tissue charring occurs much more readily when using a CO_2 laser than when operating with an Er:YAG laser [80]. Because of this limitation, many physicians prefer Er:YAG over CO_2 [45-47].

The advantages of Er:YAG soft tissue surgery are: i) Precision in ablation and coagulation; ability to use the Er:YAG laser in ablative or coagulative mode (as needed) without the risk of charring; ii) wider safety window for procedural parameters within which no tissue charring will occur iii) Less postoperative erythema. Because of the lack of thermal injury, postoperative complications are significantly reduced, and the healing is faster; and iii) Minimal risk of scarring.

In conclusion, a major limitation of the CO_2 laser is the thermal injury to the surrounding desiccated tissues, charring and melting of wound margins [76, 77, 80]. This may promote tissue defragmentation and thus frequently makes histopathological evaluation impossible. Therefore, for the majority of minor surgeries the Er:YAG laser is a better choice [76, 77].

NOTES

The authors acknowledge financial support from the state budget of the Ministry of Education, Science and Sport of Slovenia and the European Regional Development Fund (Project GOSTOP). The authors are also affiliated with Fotona d.o.o., Ljubljana, Slovenia.

REFERENCES

1. Nielsen KP et al (2008) The optics of human skin: Aspects important for human health, Solar Radiation and Human Health: 35-46.
2. Frenz M (2007) Physical Characteristics of Various Lasers Used in Stapes Surgery, Otosclerosis and Stapes Surgery. 65: 237–249.
3. Edwards GS et al (2003) Free-electron-laser-based biophysical and biomedical instrumentation. Rev. Sci. Instrum. 74 (7): 3207 – 3244.
4. Kim J et al (2013) CO_2 and Er:YAG laser interaction with grass tissues. J Appl Phys 113, 044902: 1-12.
5. Hamilton B et al (1935) The composition of tissues in dehydration. J. Biol. Chem. 1935, 109:745-753.
6. Walsh TJ et al (1989) Er:YAG laser ablation of tissue: effect of pulse duration and tissue type on thermal damage. Lasers Surg. Med. 9, 314-326.
7. Chebotareva GP et al (1996) Pulsed Photothermal Radiometry of Surgical Laser-Tissue Interaction; SPIE vol. 2681: 5-16
8. Perhavec T, Lukac M, Diaci J, Marincek M (2009) Heat Deposition of Erbium Lasers in Hard Dental Tissue; J Oral Laser Appl 9: 2015-212.
9. LeCarpentier GL et al (1993) Continuous wave laser ablation of tissue: Analysis of thermal and mechanical events. IEEE Trans. Biomed. Eng. 40, 188 -200.
10. Domankevitz Y et al (1990 Measurement of laser ablation threshold with a high-speed framing camera. IEEE J. Quantum Electron. QE-26 2276 -2278.
11. Gutknecht N. Lukac M, Marincek M, Perhavec Z, Kazic M (2011) A Novel Quantum Square Pulse (QSP) Mode Erbium Dental Laser. J LA&HA; J Laser and Health Academy, 2011(1): 15-21.
12. Majaron B, Plestenjak P, Lukac M (1999), Thermo-mechanical laser ablation of soft biological tissue: modeling the micro-explosions. Appl. Phys. B 69, 71–80.
13. Lukac M et al (2018) TightSculpting: A Complete Minimally Invasive Body Contouring Solution; Part II: Tightening with FotonaSmooth. J LA&HA; J Laser and Health Academy, 2018(1): 1-11.
14. Lukac M et al (2018) Dual Tissue Regeneration: Non-Ablative Resurfacing of Soft Tissues with FotonaSmooth Mode Er:YAG Laser. J LA&HA; J Laser and Health Academy, 2018(1): 1-17.
15. Lukac M, Perhavec T, Nemes K, Ahcan A (2010) Ablation and Thermal Depths in VSP Er:YAG Laser Skin Resurfacing. J LA&HA, J Laser and Health academy 2010(1): 56-71.
16. Walsh JT et al (1989) Er:YAG Laser Ablation of Tissue: Measurement of Ablation Rates; Lasers Surg Med 9: 327-337.
17. Hibst R et al (1991) Effects of Laser Parameters on Pulsed Er-YAG Laser Skin Ablation, Lasers in Medical Science 6(4):391-397.
18. Walsh JT et al (1988) Pulsed CO2 Laser Tissue Ablation: Measurement of the Ablation Rate: Lasers Surg Med 8:264-275
19. Venugopalan V et al (1991) The Effect of CO_2 Laser Pulse Repetition Rate on Tissue Ablation Rate and Thermal Damage; IEEE Ttansactions on Biomed Eng ; 38(9): 1049-1052.
20. Kaufmann R et al (1996) Pulsed Erbium:YAG Laser Ablation in Cutaneous Surgery, Lasers Surg Med 19:324-330.
21. Majaron B, Sustercic D, Lukac M, Skaleric U, Funduk N (1998) Heat diffusion and debris screening in Er:YAG laser ablation of hard biological tissues. Appl Phys B 66:479-487.
22. Schomacker KT et al (1990) Thermal Damage Produced by High-Irradiance Continuous Wave $C0_2$ Laser Cutting of Tissue; Lasers Surg Med 10:74-84.

23. Orvos M (2016) Rate of evaporation from the free surface of a heated liquid. Journal of Applied Mechanics and Technical Physics, 57(6): 1108–1117.
24. Hyungson K (2010) On vaporization in laser material interaction. Journal of Applied Physics 107: 104908
25. Chebotareva GP et al (1995) "Comparative study of CO2 and YAG:Er laser heating of tissue using pulsed photothermal radiometry technique; BIOS'95 SPIE vol. vol.2394: 243-251
26. Kuscer L et al (2013) Measurements of erbium laser-ablation efficiency in hard dental tissues under different water cooling conditions. J Biomed Opt. 18(10):108002
27. Lukac N, Suhovrsnik T, Lukac M, Jezersek M (2016) Ablation characteristics of quantum square pulse mode dental erbium laser. Journal of Biomedical Optics 21(1): 015012
28. Lukac M et al (2015) Investigation of the Existence of an Electromagnetically Induced Mechanical Cutting Mechanism with Er:YAG Lasers. J LA&HA - J Laser Health Acad 2015; 2015(1):OnlineFirst
29. Lukac M et al (2015) Comparison of Methods for Measuring the Ablation Efficacy of Erbium Dental Lasers. J LA&HA - J Laser Health Acad 2015; 2015(1):OnlineFirst
30. Belikov AV et al (1993) Comparative study of the 3 tm laser action on different hard tooth tissue samples using free running pulsed Er-doped YAG, YSGG, YAP and YLF lasers. SPIE Vol. 2080 Dental Applications of Lasers: 60-67
31. Diaci J et al (2012) REVIEW Comparison of Er:YAG and Er,Cr:YSGG lasers used in dentistry. . J LA&HA - J Laser Health Acad 2012(1): 1-13.
32. Riggs K, Keller M, Humphreys TR. Ablative laser resurfacing: high-energy pulsed carbon dioxide and erbium:yttrium-aluminum-garnet. Clin Dermatol. 2007;25(5):462-473.
33. Tanzi EL et al (2003) Single-Pass Carbon Dioxide Versus Multiple-Pass Er:YAG Laser Skin Resurfacing: A Comparison of Postoperative Wound Healing and Side-Effect Rates. Dermatol Surg 29:80–84 (similar results).
34. Hruza GJ (1997) Laser treatment of warts and other epidermal and dermal lesions. Lasers in Dematology 15(13): 487-504.
35. Drnovsek-Olup B et al (1997) Use of Er:YAG Laser for Benign Skin Disorders, Lasers Surg Med 21:13–19.
36. Ansari MA (2013) Mechanisms of Laser-Tissue Interaction: II. Tissue Thermal Properties. J Lasers Med Sci. 4(3): 99–106
37. McKenzie AL (1986) A three-zone model of soft-tissue damage by a CO_2 laser. Phys. Med. Biol., 31 (9): 967-983.
38. Alster TS (1999) Cutaneous resurfacing with CO_2 and Erbium:YAG lasers. Preoperative, Intraoperative, and postoperative considerations. Plastic and Reconstructive Surgery 103(2): 619-632.
39. Schwartz RJ et al (1999) Long-term assessment of CO_2 facial laser resurfacing: aesthetic results and complications. Plastic and Reconstructive Surgery 103(2): 592-601.
40. Weinstein C et al (1998) Postoperative care following carbon dioxide laser resurfacing. Avoiding pitfalls. Dermatol Surg 24:51-56.
41. Alster TS (2003) Single-pass CO_2laser skin resurfacing of light and dark skin: extended experience with 52 patients. Cosmetic & Laser Ther 5: 39-42.
42. Schoenrock LD et al (1995) Cutaneous ultrapulse laser resurfacing of the eyelids. Int J Aesthetic and Restorative Surg 3:31–36.
43. Weinstein C (1994) Ultrapulse carbon dioxide laser removal of periocular wrinkles in association with laser blepharoplasty. J Clin Laser Surg Med 12:205–209.
44. Drnovsek Olup B et al (2004) Repetitive Er:YAG laser irradiation of human skin: A histological evaluation. Lasers in Surg Med 35:146–151.
45. Stuzin JM et al (1999) CO_2 and erbium:YAG laser resurfacing: current status and personal perspective. Plast Reconstr Surg. 103(2):588-591.
46. Khatri KA, Ross V, Grevelink JM (1999) Comparison of Erbium:YAG and Carbon Dioxide Lasers in Resurfacing of Facial Rhytides. Arch Dermatol 135(4): 391-397.
47. Khatri KA (2003) Ablation of cutaneous lesions using an erbium:YAG laser. J Cosmetic & Laser Ther 5: 1–4
48. Baggish MS. Treating viral venereal infections with the CO_2 laser. J Reprod Med. 1982 Dec;27(12):737-42.
49. Meuleman C, Tomassetti C, Wolthuis A, Van Cleynenbreugel B, Laenen A, Penninckx F, Vergote I, D'Hoore A, D'Hooghe T. Clinical outcome after radical excision of moderate-severe endometriosis with or without bowel resection and reanastomosis: a prospective cohort study. Ann Surg. 2014 Mar;259(3):522-31.
50. Meuleman C, D'Hoore A, Van Cleynenbreugel B, Beks N, D'Hooghe T. (2009) Outcome after multidisciplinary CO_2 laser laparoscopic excision of deep infiltrating colorectal endometriosis. Reprod Biomed Online. 18(2):282-9.
51. Chang FH, Chou HH, Soong YK, Chang MY, Lee CL, Lai YM. Efficacy of isotopic $13CO_2$ laser laparoscopic evaporation in the treatment of infertile patients with minimal and mild endometriosis: a life table cumulative pregnancy rates study. J Am Assoc Gynecol Laparosc. 1997 Feb;4(2):219-23.
52. Chong AP, Keene ME, Thornton NL. Comparison of three modes of treatment for infertility patients with minimal pelvic endometriosis. Fertil Steril. 1990 Mar;53(3):407-10.
53. Fallani MG, Penna C, Marchionni M, Bussani C, Pieralli A, Andersson KL, Fambrini M. Prognostic significance of high-risk HPV persistence after laser CO_2 conization for high-grade CIN: a prospective clinical study. Eur J Gynaecol Oncol. 2008;29(4):378-82.
54. Békássy Z. Long-term follow-up of cervical intraepithelial neoplasia treated with minimal conization by carbon dioxide laser. Lasers Surg Med. 1997;20(4):461-6.
55. Fambrini M, Penna C, Pieralli A, Fallani MG, Andersson KL, Lozza V, Scarselli G, Marchionni M. Carbondioxide laser vaporization of the Bartholin gland cyst: a retrospective analysis on 200 cases. J Minim Invasive Gynecol. 2008 May-Jun;15(3):327-31.
56. Baumgartner J. Erbium: yttrium-aluminium-garnet (Er:YAG) laser treatment of penile pearly papules. J Cosmet Laser Ther. 2012 Jun;14(3):155-8.
57. Baumgartner J. Erbium: yttrium-aluminium-garnet (Er:YAG) laser treatment of penile pearly papules. J Cosmet Laser Ther. 2012 Jun;14(3):155-8.
58. Aynaud O, Buffet M, Roman P, Plantier F, Dupin N. Study of persistence and recurrence rates in 106 patients with condyloma and intraepithelial neoplasia after CO_2 laser treatment. Eur J Dermatol. 2008 Mar-Apr;18(2):153-8.
59. Grundsell H, Larsson G, Bekassy Z. Treatment of condylomata acuminata with the carbon dioxide laser. Br J Obstet Gynaecol. 1984 Feb;91(2):193-6.
60. Joo J, Fung MA, Jagdeo J. Successful treatment of scrotal verruciform xanthoma with shave debulking and fractionated carbon dioxide laser therapy. Dermatol Surg. 2014 Feb;40(2):214-7. doi: 10.1111/dsu.12382. Epub 2013 Dec 10.
61. Lanjouw E, de Roos KP, den Hollander JC, Prens EP. Acquired scrotal lymphangioma successfully treated using carbon dioxide laser ablation. Dermatol Surg. 2011 Apr;37(4):539-42. doi: 10.1111/j.1524-4725.2011.01914.x. Epub 2011 Mar 9.
62. Collet-Villette AM, Gaudy-Marqueste C, Grob JJ, Richard MA. [Carbon dioxide laser therapy for anogenital warts in children]. Ann Dermatol Venereol. 2007 Nov;134(11):829-32. French.
63. Treharne LJ, Murison MS (2006) CO_2 laser ablation of lymphangioma circumscriptum of the scrotum. Lymphat Res Biol. 2006;4(2):101-3.

64. Lee A, Lim A, Fischer G. Fractional carbon dioxide laser in recalcitrant vulval lichen sclerosus. Australas J Dermatol. 2015 Mar 5. doi: 10.1111/ajd.12305. [Epub ahead of print]
65. Kroft J, Shier M. A novel approach to the surgical management of clitoral phimosis. J Obstet Gynaecol Can. 2012 May;34(5):465-71.
66. Kartamaa M, Reitamo S. Treatment of lichen sclerosus with carbon dioxide laser vaporization. Br J Dermatol. 1997 Mar;136(3):356-9.
67. Baumgartner, J., 2012. Erbium: yttrium-aluminium-garnet (Er:YAG) laser treatment of penile pearly papules. Journal of cosmetic and laser therapy: official publication of the European Society for Laser Dermatology, 14(3), pp.155–158.
68. Pidal CM, Di Giorno R; Mansilla EC, San Martino JA, Narducci V, Rios VE. Resolucion quirurgica con erbium YAG laser de extensa condilomamatosis vulvar, perineal, anal e intranal.(Presented as Condilomas en clitoris. Tratamiento con Erbium YAG laser, Congreso Internacional de Patologia del tracto genital inferior y colposcopia, 1-3 Oct, 2004, Buenos Aires, Argentina)
69. Wollina, U., 2016. Erbium-YAG laser therapy – analysis of more than 1,200 treatments. Global Dermatology, 3(2), pp.268–272.
70. DiSaia PJ, Creasman WT (2012) Clinical gynecologic oncology, Elsevier Health Sciences.
71. Schellhas HS (1995) Laser surgery in gynecologic oncology. Wiley Online Library.
72. Stanton SL (2012) Principles of Gynaecological Surgery, Springer.
73. Frega A e tal (2015) Feasibility of office CO_2 laser surgery in patients affected by benign pathologies and congenital malformations of female lower genital tract. European Review for Medical and Pharmacological Sciences 19: 2528-2536
74. Apgar BS e tal (2008) Colposcopy: Principles and Practice. Elsevier Inc.
75. Merigo E et al (2013) Laser-assisted surgery with different wavelengths: a preliminary ex vivo study on thermal increase and histological evaluation. Lasers Med Sci 28:497–504
76. Błochowiak K et al (2015) Selected applications of Er:YAG and CO2 lasers for treatment of benign neoplasms and tumorous lesions in the mouth, Postep Derm Alergol XXXII (5): 337–343.
77. Suter VGA et al (2017) A randomized controlled clinical and histopathological trial comparing excisional biopsies of oral fibrous hyperplasias using CO2 and Er:YAG laser. Lasers Med Sci DOI 10.1007/s10103-017-2151-8.
78. Deckelbaum LI (1986) Use of Pulsed Energy Delivery to Minimize Tissue Injury Resulting From Carbon Dioxide Laser Irradiation of Cardiovascular Tissues. J Am Coli Cardiol 7:898-908.
79. Partovi F et al (1987) A Model for Thermal Ablation of Biological Tissue Using Laser Radiation. Lasers in Surgery and Medicine 7:141-154.
80. Stein S (1984) CO_2 Laser Surgery of the Cervix, Vagina, and Vulva. Surgical Clinics of North America- 64(5): 885-897.